Journal of Bioscience and Bioengineering
VOL. 127 No. 3, 265–272, 2019

www.elsevier.com/locate/jbiosc

Synthesis and characterization of *Ogataea thermomethanolica* alcohol oxidase immobilized on barium ferrite magnetic microparticles

Natthaya Mangkorn,[1] Pattanop Kanokratana,[2] Niran Roongsawang,[3] Apirat Laobuthee,[4] Navadol Laosiripojana,[1,5] and Verawat Champreda[2,5,*]

Joint Graduate School for Energy and Environment (JGSEE), King Mongkut's University of Technology Thonburi, Bangmod, Bangkok 10140, Thailand,[1] Enzyme Technology Laboratory, National Center for Genetic Engineering and Biotechnology, Phahonyothin Road, Khlong Luang, Pathum Thani 12120, Thailand,[2] Microbial Cell Factory Laboratory, National Center for Genetic Engineering and Biotechnology, Phahonyothin Road, Khlong Luang, Pathum Thani 12120, Thailand,[3] Department of Material Engineering, Faculty of Engineering, Kaetsart University, Chatuchak, Bangkok 10900, Thailand,[4] and JGSEE-BIOTEC Integrative Biorefinery Laboratory, National Center for Genetic Engineering and Biotechnology, Innovative Cluster 2 Building, Phahonyothin Road, Khlong Luang, Pathum Thani 12120, Thailand[5]

Received 21 May 2018; accepted 16 August 2018
Available online 20 September 2018

Alcohol oxidase catalyzes the oxidation of primary alcohols into the corresponding aldehydes, making it a potential biocatalyst in the chemical industry. However, the high production cost and poor operational stability of this enzyme are limitations for industrial application. Immobilization of enzyme onto solid supports is a useful strategy for improving enzyme stability. In this work, alcohol oxidase from the thermotolerant methylotrophic yeast *Ogataea thermomethanolica* (*Oth*AOX) was covalently immobilized onto barium ferrite ($BaFe_{12}O_{19}$) magnetic microparticles. Among different conditions tested, the highest immobilization efficiency of 71.0 % and catalytic activity of 34.6 U/g was obtained. Immobilization of *Oth*AOX onto magnetic support was shown by Fourier-Transformed infrared microscopy, scanning electron microscopy and X-ray diffraction. The immobilized *Oth*AOX worked optimally at 55 °C and pH 8.0. Immobilization also improved thermostability, in which >65% of the initial immobilized enzyme activity was retained after 24 h pre-incubation at 45 °C. The immobilized enzyme showed a greater catalytic efficiency for oxidation of methanol and ethanol than free enzyme. The immobilized enzyme could be recovered by magnetization and recycled for at least three consecutive batches, after which 70% activity remained. The properties of the immobilized enzyme suggest its potential industrial application for synthesis of aldehyde.

[**Key words:** Alcohol oxidase; Aldehyde synthesis; Immobilization; Magnetic microparticles; *Ogataea thermomethanolica*]

Aldehydes are used to produce a variety of food additives, fragrances and intermediates in the organic chemical industry (1). Currently, aldehydes and other carbonyl compounds are synthesized by energy-intensive chemical oxidation processes, which utilize harmful organic solvents and toxic metal catalysts. These processes generate large amounts of chemical by-products and waste streams (2). In recent years, oxidation of alcohols to carbonyl compounds by biocatalytic routes using alcohol dehydrogenases (ADH, EC 1.1.1.1) and oxidases (alcohol:oxygen oxidoreductase or AOX, EC 1.1.3.13) is recognized as a more environmentally friendly alternative that also has the advantages of regioselectivity and high reaction specificity (2,3). Furthermore, enzymatic processes are also operated under mild conditions which allow for facile separation of products. The biocatalytic conversion of alcohols to carbonyl compounds using ADH has been extensively studied (4); however, the reaction with ADH requires a complex regeneration of NAD-based cofactors (5). In contrast to ADH, AOX does not require an external cofactor. AOXs from methylothrophic yeasts are homo-octameric flavoproteins consisting of eight identical subunits, each containing a non-covalently bound flavin adenine dinucleotide (FAD) as a cofactor (6). AOX catalyzes the oxidation of low molecular weight alcohols by inserting molecular oxygen (O_2) into the corresponding aldehydes with the concomitant production of hydrogen peroxide (H_2O_2), while the FAD is re-oxidized to its native form during the reaction (7).

Bioconversion of alcohols to corresponding aldehydes by AOX has been reported using whole-cells from methylotrophic yeasts and purified enzyme (8–12). However, the use of free soluble AOX in industrial processes is not economically attractive owing to the high cost of enzyme production and its poor operational stability (13,14). Immobilization of enzymes is a promising strategy for enhancing their operational stability. Immobilization of AOX on solid supports by physical adsorption, covalent bonding, and entrapment has been demonstrated for biosensor applications (15–17). However, only a few reports have described immobilized AOX designs and characterized the immobilized biocatalytic properties for aldehyde synthesis (18), e.g., cross-linked enzyme aggregate (CLEA) and adsorption onto PEI-coated supports and polyurethane foam (19,20).

Recently, several types of micro- and nano-structure magnetic supports have been employed as solid matrices for enzyme immobilization (21). These magnetic supports present several

* Corresponding author at. Enzyme Technology Laboratory, National Center for Genetic Engineering and Biotechnology, Phahonyothin Road, Khlong Luang, Pathum Thani 12120, Thailand. Tel.: +66 2564 6700x3446; fax: +66 2564 6707.
E-mail address: verawat@biotec.or.th (V. Champreda).

1389-1723/$ – see front matter
https://doi.org/10.1016/j.jbiosc.2018.08.007

advantages, including high surface-to-volume ratio, easy separation of enzymes from the reaction mixture, and enzyme separation and recycling by applying an external magnetic field (22). Various forms of magnetic particles and covalent crosslinking methods have been extensively studied for preparation of different immobilized enzymes with improved catalytic performance (23). Functional silane (3-aminopropyltriethoxysilane (APTES)) with a crosslinking agent (glutaraldehyde), and activating agents, e.g., 1-ethyl-3-(3-dimethylaminopropyl) carbodiimide (EDAC), and *N*-hydroxysuccinimide (NHS) have been widely used in the modification of magnetic carriers and the enzyme surface for catalyzing various reactions (24,25). To our knowledge, there is no report on immobilization of AOX onto magnetic carriers. In this study, an AOX from *Ogataea thermomethanolica* BCC16875 (*Oth*AOX) (26) was immobilized onto magnetic microparticles of barium ferrite. *Oth*AOX is more thermostable than the corresponding enzymes from other methylotrophic yeasts, including *Pichia pastoris* (27), *Hansenula polymorpha* (27) and *Candida methanosorbosa* (28). Barium ferrite is a useful magnetic support for enzyme immobilization owing to its high chemical stability and dispersibility over the conventional Fe_3O_4 magnetic support (29,30). In addition, these physico-chemical characteristics of barium ferrite could mitigate particle agglomeration and protein aggregation problems reported for other magnetic particle forms (25,31). The physico-chemical properties of immobilized *Oth*AOX enzyme were analyzed and the catalytic performance on bioconversion of alcohols to corresponding aldehydes was evaluated. Immobilization improved the enzyme's operational stability, thus demonstrating the potential of immobilized *Oth*AOX on magnetic microparticles as a promising biocatalyst for aldehyde synthesis in the chemical industry.

MATERIALS AND METHODS

Materials *O. thermomethanolica* BCC16875 was obtained from the BIOTEC Culture Collection (www.biotec.or.th/bcc). 2,2′-Azino-bis(3-ethylbenzthiazoline-6-sulfonicacid (ABTS), horseradish peroxidase, catalase-agarose, methylbenzothiazolone hydrazone hydrochloride (MBTH) reagent and reagents for immobilized *Oth*AOX preparation [(3-aminopropyl) triethoxysilane (APTES), 1-ethyl-3-(3-dimethylaminopropyl) carbodiimide (EDC), *N*-hydroxysuccinimide (NHS), and glutaraldehyde (GA)] were purchased from Sigma–Aldrich (St. Louis, MO, USA). All reagents were analytical-grade and purchased from major chemical suppliers (e.g., Merck, Kenilworth, NJ, USA and Fluka, Seelze, Germany).

Production and purification of *Oth*AOX The purified *Oth*AOX was prepared from *O. thermomethanolica* BCC16875 as described in Mangkorn et al. (26). In brief, the cell free extract of yeast cells grown in YP-methanol medium was loaded onto a DEAE-sepharose column pre-equilibrated with 0.1 M potassium phosphate buffer, pH 7.5 on an AKTA Explorer Chromatographic system (GE Biosciences, Uppsala, Sweden). The column was washed with the same buffer, and the enzyme was eluted with an NaCl gradient. Fractions that exhibited enzyme activity were determined by the ABTS-POD method (32) and combined. The purified enzyme was dialyzed using a 30 kDa MWCO ultrafiltration column (Merck Millipore, Darmstadt, Germany). Protein concentration was determined by Bradford's method using BioRad Protein Assay Reagent (BioRad, Hercules, CA, USA) using bovine serum albumin as a protein standard.

Synthesis of $BaFe_{12}O_{19}$ magnetic supports Barium ferrite ($BaFe_{12}O_{19}$) was prepared with a modified Pechini method according to Wattanathana et al. (33). Barium nitrate Ba $(NO_3)_2$ (2.61 g), ferric nitrate Fe $(NO_3)_3 \cdot 9H_2O$ (44.53 g) in a 1:11 Ba:Fe molar ratio were first dissolved in 10 mL distilled water to obtain a clear aqueous solution. Glycerol (10 mL) was added to the solution to chelate Ba^{2+} and Fe^{3+} and form the complex precursors. The solution was heated to 120°C on a hot plate with stirring to evaporate the water until it formed very viscous brown dried gels. The dried gels were transferred to an oven and heated at 80°C for 24 h to obtain the barium hexaferrite precursor. The precursor was then calcined under the ambient atmosphere at 1000°C to obtain the powder products.

Preparation of amino-silane modified $BaFe_{12}O_{19}$ magnetic microparticles ($BaFe_{12}O_{19}$-NH_2) $BaFe_{12}O_{19}$-NH_2 microparticles were prepared using a method modified from Raita et al. (25). $BaFe_{12}O_{19}$ magnetic microparticles (0.25 g) were mixed with 0.15 mL of APTES in 4.85 mL of ethanol. This mixture was sonicated at a frequency of 35 kHz for 18 h at room temperature. Afterwards, the product was removed by magnetic separation and washed three times with 5% (v/v) ethanol solution before drying in an oven at 50°C to obtain $BaFe_{12}O_{19}$-NH_2.

Immobilization of AOX onto modified barium ferrite magnetic microparticles A 2 mL sample of purified *Oth*AOX (1 mg/mL) was mixed with 0.5 mL of 1-ethyl-3-(3-dimethylaminopropyl) carbodiimide solution (EDC) at 2.5 mg/mL and shaken in a water bath at 100 rpm for 2 h at room temperature. N-hydroxysuccinimide (NHS) (3 mg) was added to the mixture and further incubated under the same condition for 2 h. The solution was then mixed with 1 g of $BaFe_{12}O_{19}$-NH_2 microparticles and further incubated for 2 h. The immobilized *Oth*AOX was separated magnetically and then washed thrice with distilled water. Finally, the obtained immobilized enzyme, $BaFe_{12}O_{19}$- NH_2-EN-*Oth*AOX was air-dried and stored at 4°C. $BaFe_{12}O_{19}$-NH_2-EN-*Oth*AOX (0.25 g) was further crosslinked with 0.2 mL of 0.5% (v/v) glutaraldehyde (GA) solution in 25 mM potassium phosphate buffer, pH 7. The suspension was incubated at room temperature for 2 h with shaking at 100 rpm. The microparticle AOX was separated by magnetically and washed thrice with distilled water for removal of excess GA. The biocatalyst with protein crosslinking ($BaFe_{12}O_{19}$-NH_2-EN-*Oth*AOX/GA) was air-dried and stored at 4°C.

The immobilization efficiency of *Oth*AOX was determined according to Eq. 1.

$$\text{Immobilization efficiency (\%)} = \frac{\alpha_i}{\alpha_f} \times 100 \quad (1)$$

where α_i is the total activity of the immobilized enzyme and α_f is the total activity of the free enzyme.

Characterization of immobilized *Oth*AOX The functionalized magnetic microparticles and immobilized *Oth*AOX were characterized by scanning electron microscopy (SEM), Fourier-transform infrared spectroscopy (FTIR) and X-ray diffraction (XRD). The freeze dried activated magnetic carrier and immobilized enzymes were mounted on carbon tape on an aluminum stub and air dried, followed by 60 nm of gold deposition using a sputter coater. The samples were examined under SEM (XL30 series, Phillips) operating at an acceleration voltage of 13–15 kV and magnification value of ×5000. FTIR analysis of the functionalized magnetic microparticle, free *Oth*AOX, and *Oth*AOX bound barium ferrite microparticles was performed in order to confirm binding of *Oth*AOX on the microparticles. The functional groups on samples were analyzed by FTIR (Perkin–Elmer System 2000, Waltman, MA) with infrared spectra collected in the 400–4000 cm^{-1} wavenumber range. XRD data of the magnetic microparticle support and the immobilized OtAOX were collected at room temperature on a Rigaku TTRAX III X-ray diffractometer using Cu Kα radiation (λ = 1.5418 Å). Samples were scanned in the 2θ value of 10–100° at a rate of 3°/min.

Alcohol oxidase activity assay The activities of free and immobilized *Oth*AOX were determined based on the increase in absorbance at 405 nm resulting from the oxidation of ABTS by a coupled peroxidase-catalyzed reaction (ABTS-POD) according to Tani et al. (34) with some modifications. The stock mixture contained 2.8 mL of 2 mM ABTS solution (in a 100 mM potassium phosphate buffer, pH 7.5), 0.01 mL of 250 units/mL peroxidase enzyme solution, and 0.1 mL of 1% (v/v) methanol solution. The assay reaction was started by the addition of 190 μL of the stock solution with appropriate amount of free or immobilized *Oth*AOX in a microcentrifuge tube and incubated at 25°C for 1 min. The reaction was stopped by adding 13.3 μL of 4 N HCl. The immobilized enzyme was removed by centrifugation at 8000 ×*g* for 10 min. The color produced was measured spectrophotometically at 405 nm. The reading was background-corrected by subtracting the value of the blank reaction containing no enzyme. One unit of AOX was defined as the amount of enzyme that oxidized 1 μmole of methanol to formaldehyde per min at pH 7.5, 25°C.

Biochemical characterization of immobilized *Oth*AOX The effect of temperature on immobilized *Oth*AOX activity was determined based on the formation of formaldehyde at different temperatures. The reactions (1.2 mL) contained 10 mM methanol in 100 mM phosphate buffer, pH 7.5 with 0.5% (w/v) of immobilized *Oth*AOX and incubated for 10 min at different temperatures (30–70°C). The reaction was terminated by the addition of 0.04 mL of 4 N HCl, and the formaldehyde formed was determined using the Nash method. Freshly prepared Nash reagent (0.02 M acetylacetone, 0.1 M acetic acid and 3.89 M ammonium acetate) was added (0.6 mL) (35) and the reaction further incubated at 60°C for 10 min. Product was monitored spectrophotometically at 412 nm, and the product formed was determined by interpolation from the formaldehyde standard curve.

The activity of immobilized *Oth*AOX at pH 4.0 to 11.0 was determined using 10 mM methanol as a substrate under the standard assay condition (55°C). The buffers used were: 100 mM of sodium acetate (pH 4.0–6.0), potassium phosphate (pH 6.0–8.0), Tris–HCl (pH 8.0–10.0), glycine-base (pH 8.0–11.0). The formaldehyde formed was quantified using the Nash method as described above. One unit of AOX was defined as the amount of enzyme forming 1 μmole of formaldehyde per min under experimental conditions. Relative activity was calculated by comparing the activity for each treatment with that of the treatment showing maximal activity, which was designated 100%.

Thermal stability of the immobilized *Oth*AOX was determined in terms of the loss in enzyme activity when pre-incubated at 45°C in the absence of substrates. Equal amounts based on activity of free and immobilized *Oth*AOX were incubated for 3, 6, 12, and 24 h. AOX activity was determined in comparison with initial activity. The relative activity of the free and immobilized OtAOX without pre-incubation was

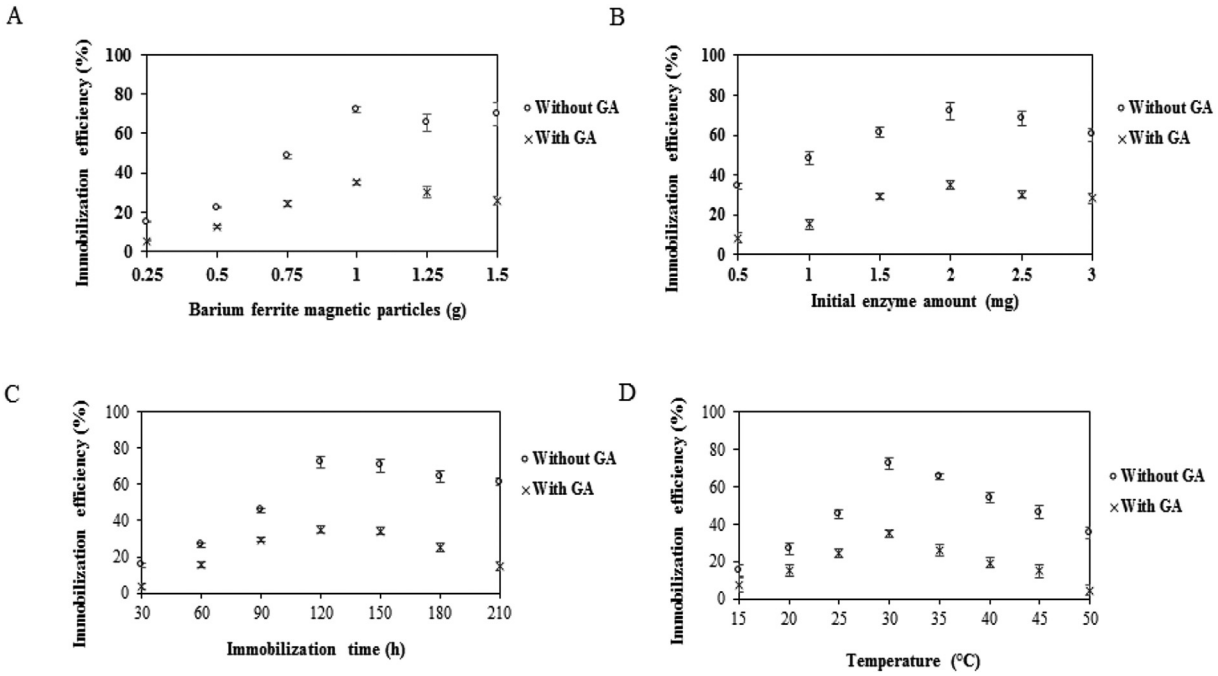

FIG. 1. Effect of immobilization parameters on immobilization efficiency of *Oth*AOX. (A) amount of barium ferrite magnetic, (B) initial enzyme amount, (C) immobilization time, (D) immobilization temperature. The data represent averages from triplicate experiments.

defined as the control and designated as 100% relative activity for each of their respective reactions.

The substrate specificities of immobilized *Oth*AOX were determined by ABTS-POD assay using 1% (v/v) alcohol substrate. The alcohols (methanol, ethanol, 1-propanol, 1-butanol, 1-pentanol, 1-hexanol, 1-octanol, 2-propanol, *tert*-butanol, 3-pentanol, 3-methyl-1-butanol, and glycerol) were incubated with 0.5% (w/v) immobilized enzyme in phosphate buffer pH 7.5 at 30°C for 10 min. Relative activity was calculated by comparing the activity for each substrate with that of the reaction showing maximal activity, which was designated 100%.

The kinetic parameters (K_m, and V_{max}) of immobilized AOX were determined using the ABTS-POD method at various concentrations of the substrates by fitting the initial velocity data to the Michaelis–Menten equation using Kaleida Graph data analysis software (Synergy Software, Reading, PA, USA).

Bioconversion of ethanol to acetaldehyde The oxidation reaction was conducted in screw-capped serum vials in order to prevent the loss of volatile substances. The reaction (10 mL) was initiated by adding 0.5% (w/v) of ethanol solution in 0.1 M Tris buffer (pH 8), 1% (w/v) of immobilized *Oth*AOX, and 0.01% (w/v) catalase-agarose. The reaction was incubated at 30°C with shaking at 180 rpm for 8 h. The oxidation efficiency was followed at different time points by the MBTH assay.

Aldehyde determination by MBTH assay Aldehyde products were quantified by the MBTH assay as described previously (35) with some modifications. The assay contained 100 µL of 100 mM Tris–HCl buffer, pH 6, 50 µL of 3 mg/mL MBTH, and 50 µL of sample or H_2O. The reaction was incubated for 15 min at 30°C, and then 200 µL of a solution containing 5 mg/mL each of ferric ammonium sulfate and sulfamic acid was added. After 20 min at room temperature, 0.6 mL of H_2O was added to obtain a final volume of 1.0 mL, and absorbance at 620 nm was measured.

RESULTS AND DISCUSSION

Preparation of immobilized *Oth*AOX *Oth*AOX was immobilized on $BaFe_{12}O_{19}$ magnetic microparticles as the solid carrier through covalent linkages. The pre-concentrated *Oth*AOX solution had a specific activity of 14.5 unit/mg protein using methanol as a substrate. The surface of barium ferrite magnetic microparticles was functionalized with APTES by silanization to obtain amino functionalized magnetic microparticles. APTES was covalently bound to the surface of magnetic microparticles through a condensation reaction to obtain $BaFe_{12}O_{19}$-NH_2. Immobilization of *Oth*AOX was done by linking the carboxyl groups of *Oth*AOX activated by EDC and NHS to the amino group of $BaFe_{12}O_{19}$-NH_2 to obtain $BaFe_{12}O_{19}$-NH_2-EN-*Oth*AOX. The proteins on the surface were optionally further crosslinked by GA to obtain $BaFe_{12}O_{19}$-NH_2-EN/GA-*Oth*AOX. The schematic diagram on the enzyme immobilization is shown in Fig. S1.

To evaluate the optimal conditions of *Oth*AOX immobilization, several interdependent parameters that could influence the immobilization efficiency were investigated (Fig. 1). Enzyme immobilization was performed using different amounts of barium ferrite magnetic support (0.25–1 g) at a fixed enzyme loading (2 mg/mL) and immobilization time as shown in Fig. 1A. The

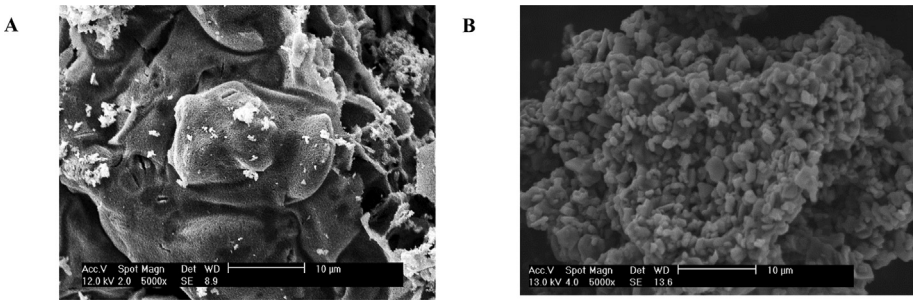

FIG. 2. SEM analysis of protein-free microparticle supports (A) and immobilized *Oth*AOX $BaFe_{12}O_{19}$-NH_2-EN-*Oth*AOX (B).

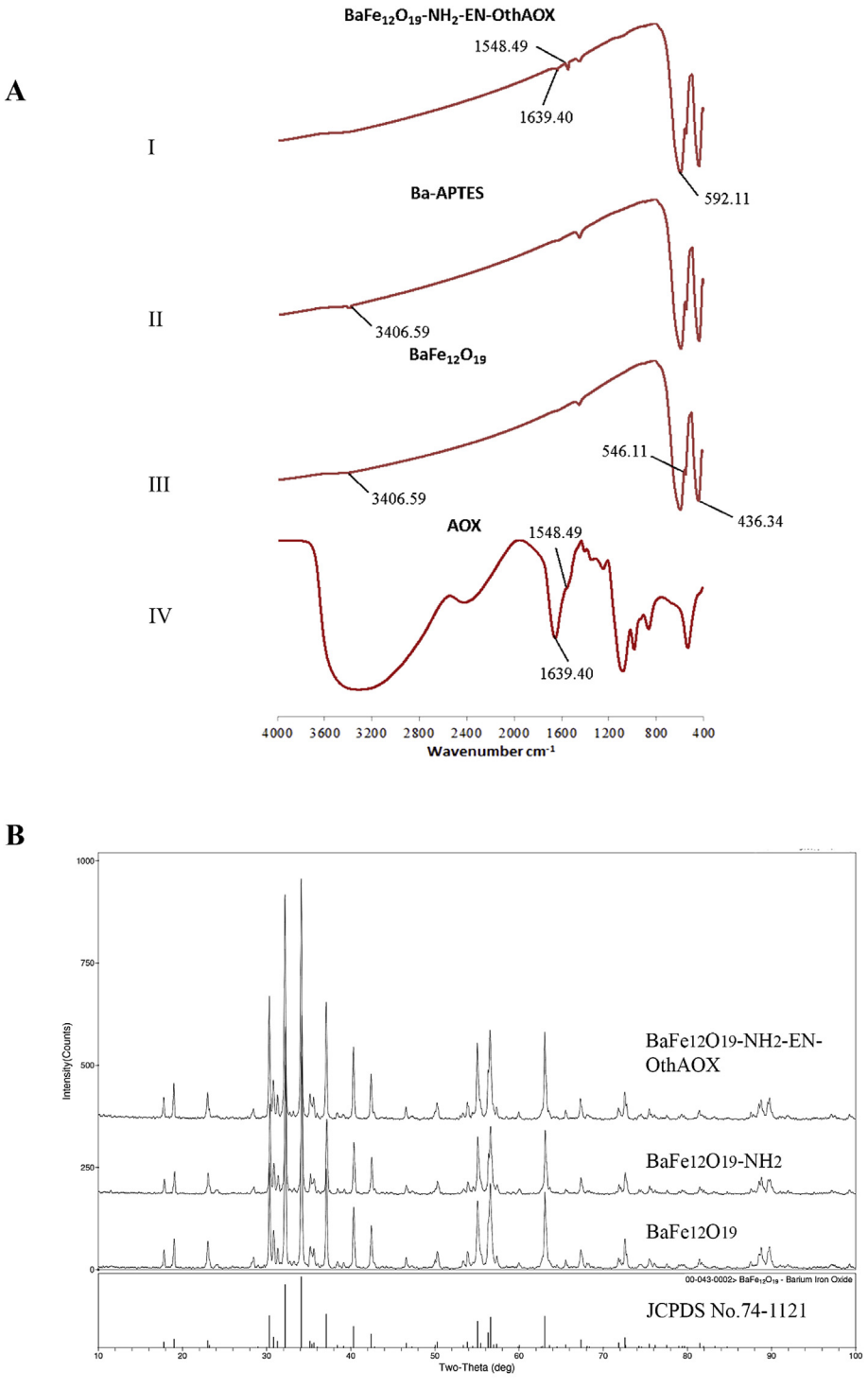

FIG. 3. Physicochemical analysis of immobilized *Oth*AOX. (A) FT-IR spectra of free *Oth*AOX, barium ferrite microparticle matrices with and without surface modification and different forms of immobilized *Oth*AOX; (I) $BaFe_{12}O_{19}$-NH_2-EN-*Oth*AOX, (II) $BaFe_{12}O_{19}$-NH_2, (III) $BaFe_{12}O_{19}$ and (IV) *Oth*AOX; (B) XRD patterns of barium ferrite microparticles with and without enzyme.

immobilization efficiency was enhanced by increasing the amount of barium ferrite, reaching a maximum at 1 g of magnetic support. Immobilization efficiency was also enhanced by increasing the initial amount of enzyme up to a maximum with 2 mg of enzyme (Fig. 1B). Initial amounts of enzyme greater than 2 mg did not produce more active biocatalyst, probably because the protein binding sites were saturated on the surface of the magnetic carriers. Excessive loading of enzyme can lead to over-accumulation of enzyme on the magnetic carrier, resulting in steric hindrance, loss of structural flexibility required for catalysis and decrease in immobilization efficiency (36). The immobilization time also influenced the activity of immobilized *Oth*AOX (Fig. 1C). The immobilization efficiency increased with immobilization time, reaching a maximum within 2 h and declining thereafter. The immobilization efficiency was assessed at different immobilization temperatures (Fig. 1D). The immobilization efficiency increased

with increasing temperatures in the range of 15–30°C, and decreased rapidly at higher temperatures. The lower efficiency at temperatures greater than 30°C is suggestive of enzyme inactivation under these conditions. The maximum immobilization efficiency of 71.0 % $BaFe_{12}O_{19}$-NH_2-EN-*Oth*AOX or 73.6% based on total protein recovery was obtained from the condition using 1 g of barium ferrite magnetic support, 2 mg of *Oth*AOX, at 30°C for 2 h. Enzyme activity was lower for immobilizations conducted with GA cross-linking (Fig. 1A–D), suggesting that cross-linking causes excess intramolecular and intermolecular interactions within and between the enzyme molecules bound on the biocatalyst's surface, which increase enzyme rigidity and cause loss of structural flexibility required for catalysis (37). In addition, the partial distortion of the enzyme's overall structure caused by cross-linking could affect the active site conformation and thus reduce catalytic efficiency of the immobilized enzymes (38). The immobilized *Oth*AOX ($BaFe_{12}O_{19}$-NH_2-EN-*Oth*AOX) showed a catalytic activity of 34.6 U/g, equivalent to a specific activity of 10.3 U/mg protein immobilized on the solid support. The decrease in specific activity upon immobilization could be due to partial enzyme inactivation and alteration in the enzyme's molecular structure caused by chemical reactions during the immobilization process (39).

Physical characterization of immobilized *Oth*AOX Magnetic microparticle morphology was investigated by SEM (Fig. 2). The protein-free barium ferrite microparticle support ($BaFe_{12}O_{19}$) showed well-defined ultrafine powder structures with plate-like shaped, smooth-surface particles of 0.39 μm average diameter. The SEM images of magnetic microparticle linked with *Oth*AOX clearly showed a typical agglomeration of magnetic microparticles with a rough protein surface. FT-IR analysis revealed covalent binding of *Oth*AOX on the barium ferrite microparticles (Fig. 3A). The FT-IR spectra of free *Oth*AOX showed a signature peak at 1639.40 cm^{-1} for the amide I band due to C=O stretching vibrations of the peptide bonds and a peak at 1548.49 cm^{-1} for amide II from N–H bending vibration (40,41). The strong absorption peaks at 592.11 cm^{-1}, 546.11 cm^{-1}, and 436.34 cm^{-1} (31,42) are assigned to Fe–O stretching vibrations of hexaferrite in $BaFe_{12}O_{19}$ and $BaFe_{12}O_{19}$-NH_2. These spectra are similar to those reported for barium ferrite microparticle support by Meng et al. (43). The hydroxyl absorption peak (O–H stretching vibration) of $BaFe_{12}O_{19}$ microparticle support was observed near 3393.40 cm^{-1}. The broad band at 3406.59 cm^{-1} was attributed to the free NH_2 groups (N–H stretching vibration) which overlapped the O–H stretching vibration. These results suggest that NH_2 groups were successfully attached to the surface of $BaFe_{12}O_{19}$ microparticles (24). The spectrum of $BaFe_{12}O_{19}$-NH_2-EN-*Oth*AOX showed the combination of signature peaks of both *Oth*AOX and the magnetic microparticle matrix. The characteristic peaks of protein for amide I and II were present in the pure *Oth*AOX and *Oth*AOX bound microparticle support. This indicated that *Oth*AOX was successfully bound to the carrier (44,45). The immobilized *Oth*AOX showed the same XRD pattern as the protein-free $BaFe_{12}O_{19}$ matrix (Fig. 3B); hence, immobilization of *Oth*AOX did not induce any structural change in the barium iron oxide particles.

Biochemical characterization of immobilized *Oth*AOX The effect of varying temperature and pH on the activity of immobilized *Oth*AOX were investigated. The optimal temperature of the immobilized enzyme was 55°C. The immobilized enzyme also retained approximately 60 % of its maximal activity at 60°C, which was markedly higher than that of the free *Oth*AOX (Fig. 4A). Thermostability of the immobilized *Oth*AOX pre-incubated at 45°C was assessed by measuring the remaining enzyme activity (Fig. 4B). The immobilized enzyme retained more than 65% of its initial activity after 24 h pre-incubation. In contrast, the free *Oth*AOX retained only 15% activity under the same condition. The increased thermostability of the immobilized enzyme could be attributed to formation of multiple covalent bridges between the protein molecules and magnetic support which could reduce conformational mobility in the enzyme's structure and denaturation at higher temperatures (46,47). These covalent attachments led to more resistant on unfolding of the enzyme molecules when exposed to higher temperature and thus higher thermodynamic stability of the immobilized enzyme (48,49). The immobilized *Oth*AOX showed optimal activity at pH 8.0, with >75% activity in the pH range of 6–9, which was not markedly different from the free enzyme (Fig. 4C).

The catalytic activities of immobilized *Oth*AOX against different aliphatic alcohols are shown in Table 2. Among the tested substrates, the immobilized AOX showed the highest activity on methanol. Activity on primary alcohols decreased with increasing alkyl chain length. Secondary (2-propanol and 3-pentanol) alcohols were oxidized at much lower rates than the primary alcohols. The substrate specificity of immobilized *Oth*AOX is the same as that reported for free AOX enzymes, which show the highest specificity towards short-chain aliphatic alcohols (6). Kinetic studies of

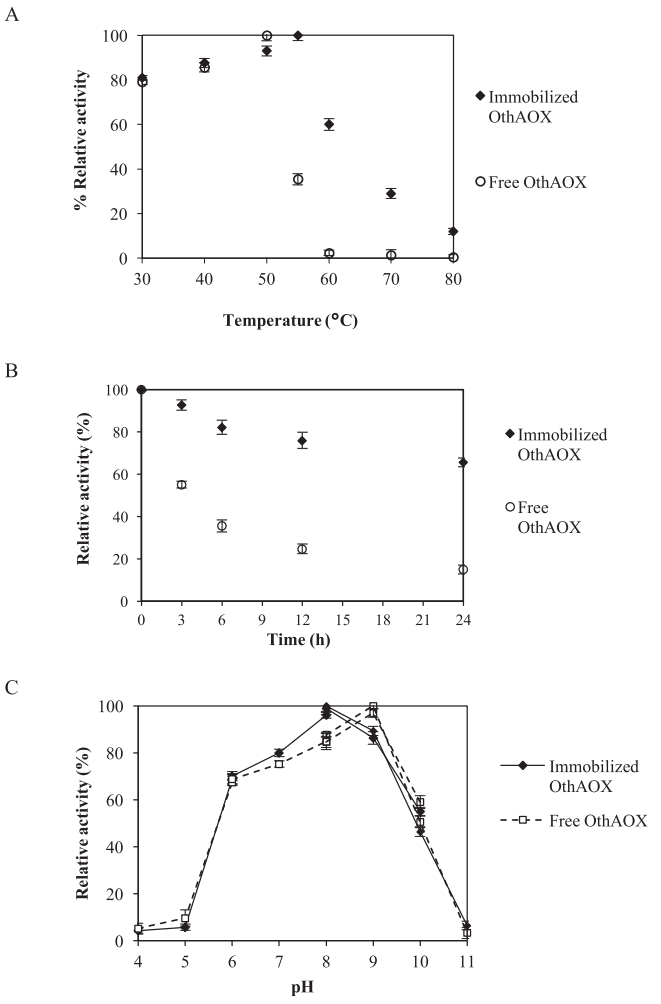

FIG. 4. Effects of temperature, thermostability and pH on activity of free and immobilized *Oth*AOX. (A) Temperature: The reactions contained 10 mM methanol in 100 mM phosphate buffer, pH 7.5 with 0.5% (w/v) immobilized enzyme and incubated at varying temperature for 10 min. (B) Thermostability: the residual activity was measured after pre-incubation at 45°C for 3, 6, 12, and 24 h at different temperatures. (C) pH: The reactions contained 10 mM methanol in different buffers with 0.5% (w/v) immobilized enzyme and incubated at 55°C for 10 min. The data represent averages from triplicate experiments. Data for free *Oth*AOX are referred from Mangkorn et al. (26).

TABLE 1. Comparison of biochemical characteristics of different immobilized AOX.

Source of AOX	Immobilization support	Optimal temperature (°C) and pH	Thermostability (% of initial activity at different temperature (°C)	Reference
O. thermomethanolica	Barium ferrite magnetic microparticles	55, pH 8	>65 (45 °C, 24 h)	This study
P. pastoris	Electrospun polystyrene-co-maleic anhydride fibers with poly(ethylene glycol) diamine	50, pH 6.5	>40 (45 °C, 24 h)	47
P. pastoris	Polypyrrole (PPy)	40, pH 8	n.d.	7
P. pastoris	CP-copolypyrrole matrices	50, pH 9	n.d.	7
P. pastoris	Polypyrrole (PPy), poly(3,4-ethylenedioxythiophene) (PEDOT), and poly(3,4-ethylenedioxypyrrole) (PEDOP)	40, pH 7	n.d.	50
P. pastoris	Agarose coated with polyethyleneimine	n.d.	>40 (45 °C, 24 h)	15
Hansenula sp.	MANAE agarose	n.d.	>40 (45 °C, 24 h)	15
P. pastoris	Cross-linked enzyme aggregates (CLEA)	40, pH 6	>60 (45 °C, 30 min)	19

immobilized AOX were performed on methanol and ethanol substrates at 30°C (Fig. S2). The immobilized *Oth*AOX showed a K_m of 0.21 mM with maximal velocity (V_{max}) of 3.09 nmol/min against methanol, whereas the maximal velocity of 2.20 nmol/min and K_m of 0.81 mM were observed on ethanol (Table S1). Compared with free *Oth*AOX, the immobilized *Oth*AOX showed slightly change in K_m against methanol but markedly lower K_m against ethanol ($p < 0.05$ according to t-test), suggesting higher affinity towards the longer alcohol. The significantly higher V_{max} of the immobilized enzyme compared with free enzyme (12.8 and 5.4 fold on methanol and ethanol, respectively) was thus primarily responsible for the marked enhancement on the catalytic efficiency (k_{cat}/K_m) to 27,812 and 6166 min^{-1} mM^{-1} against methanol and ethanol, respectively (2.0 and 5.3 folds, respectively, compared to free enzyme). The results thus suggest that the immobilized enzyme has superior catalytic performance to the free enzyme under the experimental conditions.

According to Table 1, the immobilized *Oth*AOX showed higher optimal temperature and thermostability to previously reported immobilized AOX enzymes from different microbial origins using different immobilization techniques (7,15,19,47,50). This reflected the higher intrinsic stability of *Oth*AOX and advantages of the covalent immobilization methods on magnetic support in this study and thus suggested higher operational stability of the immobilized *Oth*AOX in the aldehyde synthesis process.

Bioconversion of ethanol to acetaldehyde The conversion of ethanol to acetaldehyde was tested using immobilized *Oth*AOX in small-scale batch vials at 30°C. Ethanol was efficiently converted to acetaldehyde with a yield of 75.3% after 6 h of oxidation reaction in Tris buffer system (Fig. 5A). An alkaline Tris buffer was used in the reaction to prevent end-product inhibition of immobilized *Oth*AOX (51). The pH of the reaction was reduced in order to release the acetaldehyde that was produced during the reaction from the Tris-aldehyde complex formed at pH 8. The formation of acetaldehyde was slow, requiring 6 h incubation to reach maximum yield. This could be due to the limited binding capacity of Tris (equilibrium constant = 0.2) (52), such that enzyme inhibition by free acetaldehyde becomes significant after prolonged incubation. The slow formation of aldehyde could also be due to the limited capacity of catalase to remove inhibitory H_2O_2 from the reaction (53). The amount of acetaldehyde

TABLE 2. Substrate specificity of immobilized *Oth*AOX.

Substrate	Relative activity (%)
Methanol	100.00 ± 0.20
Ethanol	82.32 ± 0.21
1-Propanol	50.34 ± 0.55
1-Butanol	23.45 ± 0.79
1-Pentanol	1.74 ± 1.21
1-Hexanol	0.27 ± 0.45
1-Octanol	0.19 ± 0.89
2-Propanol	0.95 ± 0.75
3-Pentanol	0.43 ± 0.45
3-Methyl-1-butanol	0.12 ± 0.67
Glycerol	0.15 ± 0.14

The data represent averages from triplicate experiments.

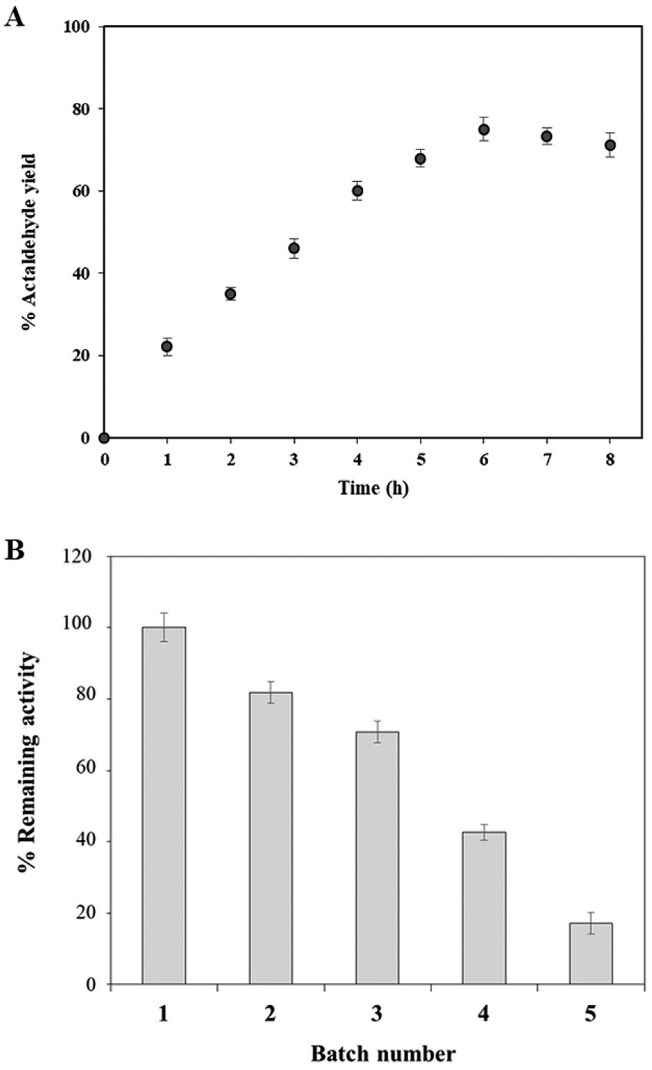

FIG. 5. Conversion of acetaldehyde to ethanol. (A) Reaction profile for oxidation of ethanol to acetaldehyde. The reactions were done in glass vials with the following conditions: 0.5% (w/v) of ethanol solution in 0.1 M Tris buffer (pH 8), 1% (w/v) of immobilized *Oth*AOX, and 0.01% (w/v) catalase-agarose and incubated at 30°C, 180 rpm for 8 h. (B) Reusability of the magnetic microparticle *Oth*AOX in consecutive batch process. The biocatalyst was separated by magnetization after each incubation cycle and washed with 0.1 M Tris–HCl buffer (pH 8) before reuse. The remaining activity was calculated based on the acetaldehyde yield divided by the initial acetaldehyde yield from the first batch. The data represent averages from triplicate experiments.

produced in the reaction catalyzed by the immobilized *Oth*AOX was more than twice that reported previously using cross-linked enzyme aggregates AOX from *P. pastoris* for oxidization of 100 mM 1-propanol, in which only 20% of product yield was obtained after 3 h (19). A maximum yield of *n*-heptanal of 20.7 ± 1.2 % (w/w) was obtained using 10 mM *n*-heptanol and decreased to 1.2 ± 0.1 % (w/w) with the increasing *n*-heptanol concentration of 40 mM using AOX from *Aspergillus terreus* immobilized on polyurethane foam matrix (20). However, it should be noted that the poorer substrates were used which might cause lower product yields according to these previous studies.

Reusability of the immobilized *Oth*AOX The reusability of $BaFe_{12}O_{19}$-NH_2-EN-*Oth*AOX was studied by analyzing the conversion efficiency after consecutive batch cycles (Fig. 5B). The biocatalyst was recovered and washed with 0.1 M Tris−HCl (pH 8) buffer before reusing in the next batch without further reactivation. The biocatalyst retained high operational stability after repeated use, with approximately 70% of the original activity remaining after three consecutive batch cycles under experimental conditions. This result thus demonstrates the potential of the biocatalyst in the consecutive batch process.

In conclusion, *Oth*AOX was successfully immobilized on barium ferrite magnetic microparticles. The immobilized enzyme showed high potential for use as a biocatalyst for conversion of alcohols to corresponding aldehydes. The immobilized *Oth*AOX showed higher optimal temperature and improved thermal stability compared with the free enzyme. Furthermore, the immobilized enzyme could be recovered by simple magnetic separation, and was demonstrated to retain activity after consecutive batch cycles. The superior properties of the immobilized enzyme could lead to cost reductions in the production of aldehydes with improved economic feasibility.

Supplementary data related to this article can be found at https://doi.org/10.1016/j.jbiosc.2018.08.007.

ACKNOWLEDGMENTS

This project was financially supported by a research grant from Thailand Research Fund (RTA5980006) and the National Science and Technology Development Agency (P-15-50502). NM was financially supported by the Royal Golden Jubilee scholarship (PHD 0164′2554). Manuscript proofreading by Dr. Phillip J. Shaw is highly appreciated. The authors have no conflict of interest to declare.

References

1. **Augugliaro, V. and Palmisano, L.:** Green oxidation of alcohols to carbonyl compounds by heterogeneous photocatalysis, ChemSusChem, **3**, 1135−1138 (2010).
2. **Hirano, J.-i., Miyamoto, K., and Ohta, H.:** The green and effective oxidation of alcohols to carboxylic acids with molecular oxygen via biocatalytic reaction, Tetrahedron Lett., **49**, 1217−1219 (2008).
3. **Turner, N. J.:** Enantioselective oxidation of C−O and C−N bonds using oxidases, Chem. Rev., **111**, 4073−4087 (2011).
4. **Hollmann, F., Arends, I. W. C. E., Buehler, K., Schallmey, A., and Buhler, B.:** Enzyme-mediated oxidations for the chemist, Green Chem., **13**, 226−265 (2011).
5. **Kroutil, W., Mang, H., Edegger, K., and Faber, K.:** Biocatalytic oxidation of primary and secondary alcohols, Adv. Synth. Catal., **346**, 125−142 (2004).
6. **Goswami, P., Chinnadayyala, S. S. R., Chakraborty, M., Kumar, A. K., and Kakoti, A.:** An overview on alcohol oxidases and their potential applications, Appl. Microbiol. Biotechnol., **97**, 4259−4275 (2013).
7. **Yildiz, H. B. and Toppare, L.:** Biosensing approach for alcohol determination using immobilized alcohol oxidase, Biosens. Bioelectron., **21**, 2306−2310 (2006).
8. **Duff, S. J. B. and Murray, W. D.:** Oxidation of benzyl alcohol by whole cells of *Pichia pastoris* and by alcohol oxidase in aqueous and nonaqueous reaction media, Biotechnol. Bioeng., **34**, 153−159 (1989).
9. **Murray, W. D. and Duff, S. J. B.:** Bio-oxidation of aliphatic and aromatic high molecular weight alcohols by *Pichia pastoris* alcohol oxidase, Appl. Microbiol. Biotechnol., **33**, 202−205 (1990).
10. **Duff, S. J. B. and Murray, W. D.:** Production and application of methylotrophic yeast *Pichia pastoris*, Biotechnol. Bioeng., **31**, 44−49 (1988).
11. **Moroz, O. M., Gonchar, M. V., and Sibirny, A. A.:** Efficient bioconversion of ethanol to acetaldehyde using a novel mutant strain of the methylotrophic yeast *Hansenula polymorpha*, Biotechnol. Bioeng., **68**, 44−51 (2000).
12. **Clark, D. S., Geresh, S., and DiCosimo, R.:** Enantioselective oxidation of 2-methyl-1-alkanols by alcohol oxidase from methylotrophic yeasts, Bioorg. Med. Chem. Lett, **5**, 1383−1388 (1995).
13. **Duff, S. J. B. and Murray, W. D.:** Comparison of free and immobilized *Pichia pastoris* cells for conversion of ethanol to acetaldehyde, Biotechnol. Bioeng., **31**, 790−795 (1988).
14. **Maleknia, S., Ahmadi, H., and Norouzian, D.:** Immobilization of *Pichia pastoris* cells containing alcohol oxidase activity, Iran. J. Microbiol., **3**, 210−215 (2011).
15. **Lopez-Gallego, F., Betancor, L., Hidalgo, A., Dellamora-Ortiz, G., Mateo, C., Fernández-Lafuente, R., and Guisán, J. M.:** Stabilization of different alcohol oxidases via immobilization and post immobilization techniques, Enzyme Microb. Technol., **40**, 278−284 (2007).
16. **Yildiz, H. B., Sahmetlioglu, E., Boyukbayram, A. E., Toppare, L., and Yagci, Y.:** Immobilization of tyrosinase and alcohol oxidase in conducting copolymers of thiophene functionalized poly(vinyl alcohol) with pyrrole, Int. J. Biol. Macromol., **41**, 332−337 (2007).
17. **Kuswandi, B., Irmawati, T., Hidayat, M. A., Jayus, and Ahmad, M.:** A simple visual ethanol biosensor based on alcohol oxidase immobilized onto polyaniline film for halal verification of fermented beverage samples, Sensors (Basel, Switzerland), **14**, 2135−2149 (2014).
18. **Dienys, G., Jarmalavicius, S., Budriene, S., Citavicius, D., and Sereikaite, J.:** Alcohol oxidase from the yeast *Pichia pastoris*—a potential catalyst for organic synthesis, J. Mol. Catal. B Enzym., **21**, 47−49 (2003).
19. **Gruškienė, R. t., Kairys, V., and Matijošytė, I.:** CLEA-based immobilization of methylotropic yeast alcohol oxidase: influence on storage stability and reaction efficiency, Org. Process Res. Dev., **19**, 2025−2033 (2015).
20. **Kakoti, A., Kumar, A. K., and Goswami, P.:** Microsome-bound alcohol oxidase catalyzed production of carbonyl compounds from alcohol substrates, J. Mol. Catal. B Enzym., **78**, 98−104 (2012).
21. **Yiu, H. H. P. and Keane, M. A.:** Enzyme−magnetic nanoparticle hybrids: new effective catalysts for the production of high value chemicals, J. Chem. Technol. Biotechnol., **87**, 583−594 (2012).
22. **Conde, J., Dias, J. T., Grazú, V., Moros, M., Baptista, P. V., and de la Fuente, J. M.:** Revisiting 30 years of biofunctionalization and surface chemistry of inorganic nanoparticles for nanomedicine, Front. Chem., **2**, 48 (2014).
23. **Ahmad, R.,S. M.:** Enzyme immobilization: an overview on nanoparticles as immobilization matrix, Biochem. Anal. Biochem., **4**, 178 (2015).
24. **Safari, J. and Zarnegar, Z.:** Ultrasonic activated efficient synthesis of chromenes using amino-silane modified Fe3O4 nanoparticles: a versatile integration of high catalytic activity and facile recovery, J. Mol. Struct., **1072**, 53−60 (2014).
25. **Raita, M., Arnthong, J., Champreda, V., and Laosiripojana, N.:** Modification of magnetic nanoparticle lipase designs for biodiesel production from palm oil, Fuel Process. Technol., **134**, 189−197 (2015).
26. **Mangkorn, N., Kanokratana, P., Roongsawang, N., Laosiripojana, N., and Champreda, V.:** Purification, characterization, and stabilization of alcohol oxidase from *Ogataea thermomethanolica*, Protein Expr. Purif., **150**, 26−32 (2018).
27. **Couderc, R. and Baratti, J.:** Oxidation of methanol by the yeast, *Pichia pastoris*. Purification and properties of the alcohol oxidase, Agric. Biol. Chem., **44**, 2279−2289 (1980).
28. **Suye, S.-i.:** Purification and properties of alcohol oxidase from *Candida methanosorbosa* M-2003, Curr. Microbiol., **34**, 374−377 (1997).
29. **El-Batal, A. I., Farrag, A. A., Elsayed, M. A., and El-Khawaga, A. M.:** Biodiesel production by *Aspergillus niger* lipase immobilized on barium ferrite magnetic nanoparticles, Bioengineering, **3**, 14 (2016).
30. **Liu, X., Wang, J., Gan, L.-M., and Ng, S.-C.:** Improving the magnetic properties of hydrothermally synthesized barium ferrite, J. Magn. Magn. Mater., **195**, 452−459 (1999).
31. **Bordbar, A. K., Rastegari, A. A., Amiri, R., Ranjbakhsh, E., Abbasi, M., and Khosropour, A. R.:** Characterization of modified magnetite nanoparticles for albumin immobilization, Biotechnol. Res. Int., **2014**, 705068 (2014).
32. **Tani, Y., Miya, T., Nishikawa, H., and Ogata, K.:** The microbial metabolism of methanol, Agric. Biol. Chem., **36**, 68−83 (1972).
33. **Wattanathana, W., Nantharak, W., Wannapaiboon, S., Jantaratana, P., Veranitisagul, C., Koonsaeng, N., and Laobuthee, A.:** Barium ferrite prepared by modified Pechini method: effects of chloride and nitrate counter ions on microstructures and magnetic properties, J. Mater. Sci. Mater. Electron., **29**, 1542−1553 (2018).
34. **Tani, Y., Sakai, Y., and Yamada, H.:** Isolation and characterization of a mutant of a methanol yeast, *Candida boidinii* S2, with higher formaldehyde productivity, Agric. Biol. Chem., **49**, 2699−2706 (1985).
35. **Anthon, G. E. and Barrett, D. M.:** Comparison of three colorimetric reagents in the determination of methanol with alcohol oxidase. Application to the assay of pectin methylesterase, J. Agric. Food Chem., **52**, 3749−3753 (2004).
36. **Qiu, G. M., Zhu, B. K., and Xu, Y. Y.:** α-Amylase immobilized by Fe_3O_4/poly(-styrene-co-maleic anhydride) magnetic composite microspheres: preparation and characterization, J. Appl. Polym. Sci., **95**, 328−335 (2005).

37. **Barbosa, O., Torres, R., Ortiz, C., and Fernandez-Lafuente, R.:** The slow-down of the CALB immobilization rate permits to control the inter and intra molecular modification produced by glutaraldehyde, Process Biochem., **47**, 766–774 (2012).
38. **Chui, W. K. and Wan, L. S. C.:** Prolonged retention of cross-linked trypsin in calcium alginate microspheres, J. Microencapsul., **14**, 51–61 (1997).
39. **Prasertpornsakun, N., Raita, M., Laosiripojana, N., and Champreda, V.:** Biocatalytic synthesis of starch esters by immobilized lipase on magnetic microparticles, Biosci. Biotechnol. Biochem., **79**, 1750–1758 (2015).
40. **Cao, H., He, J., Deng, L., and Gao, X.:** Fabrication of cyclodextrin-functionalized superparamagnetic Fe_3O_4/amino-silane core–shell nanoparticles via layer-by-layer method, Appl. Surf. Sci., **255**, 7974–7980 (2009).
41. **Lin, J., Zhao, B., Cao, Y., Xu, H., Ma, S., Guo, M., Qiao, D., and Cao, Y.:** Rationally designed Fe-MCM-41 by protein size to enhance lipase immobilization, catalytic efficiency and performance, Appl. Catal. Gen., **478**, 175–185 (2014).
42. **Zang, X. and Xie, W.:** Enzymatic interesterification of soybean oil and methyl stearate blends using lipase immobilized on magnetic Fe_3O_4/SBA-15 composites as a biocatalyst, J. Oleo Sci., **63**, 1027–1034 (2014).
43. **Meng, Y. Y., He, M. H., Zeng, Q., Jiao, D. L., Shukla, S., Ramanujan, R. V., and Liu, Z. W.:** Synthesis of barium ferrite ultrafine powders by a sol–gel combustion method using glycine gels, J. Alloy. Comp., **583**, 220–225 (2014).
44. **Ashtari, K., Khajeh, K., Fasihi, J., Ashtari, P., Ramazani, A., and Vali, H.:** Silica-encapsulated magnetic nanoparticles: enzyme immobilization and cytotoxic study, Int. J. Biol. Macromol., **50**, 1063–1069 (2012).
45. **Xie, W. and Zang, X.:** Immobilized lipase on core–shell structured Fe_3O_4–MCM-41 nanocomposites as a magnetically recyclable biocatalyst for interesterification of soybean oil and lard, Food Chem., **194**, 1283–1292 (2016).
46. **Zhu, J. and Sun, G.:** Lipase immobilization on glutaraldehyde-activated nanofibrous membranes for improved enzyme stabilities and activities, React. Funct. Polym., **72**, 839–845 (2012).
47. **Zhao, L., Liu, Q., Yan, S., Chen, Z., Chen, J., and Li, X.:** Multimeric immobilization of alcohol oxidase on electrospun fibers for valid tests of alcoholic saliva, J. Biotechnol., **168**, 46–54 (2013).
48. **Verma, M. L., Chaudhary, R., Tsuzuki, T., Barrow, C. J., and Puri, M.:** Immobilization of β-glucosidase on a magnetic nanoparticle improves thermostability: application in cellobiose hydrolysis, Bioresour. Technol., **135**, 2–6 (2013).
49. **Karam, E. A., Abdel Wahab, W. A., Saleh, S. A. A., Hassan, M. E., Kansoh, A. L., and Esawy, M. A.:** Production, immobilization and thermodynamic studies of free and immobilized *Aspergillus awamori* amylase, Int. J. Biol. Macromol., **102**, 694–703 (2017).
50. **Türkarslan, Ö., Böyükbayram, A. E., and Toppare, L.:** Amperometric alcohol biosensors based on conducting polymers: polypyrrole, poly(3,4-ethylenedioxythiophene) and poly(3,4-ethylenedioxypyrrole), Synth. Met., **160**, 808–813 (2010).
51. **Murray, W. D., Duff, S. J. B., and Lanthier, P. H.:** Induction and stability of alcohol oxidase in the methylotrophic yeast *Pichia pastoris*, Appl. Microbiol. Biotechnol., **32**, 95–100 (1989).
52. **John, L., Palmer, M. W. T., and Daubney, S. D.:** Acetaldehyde trapping system, US5112741A (1992).
53. **Maha, K. C., Sylviane, P., Abdelghani, M., Daniel, T., Didier, T., and Werner, K.:** Biooxidation of *n*-hexanol by alcohol oxidase and catalase in biphasic and micellar systems without solvent, Biotechnol. Bioeng., **81**, 27–32 (2003).